Inorganic Chemistry

ARTICLE

pubs.acs.org/IC

New Type of Heterometallic 3d−4f Rhomblike Core in Weakley-Like Polyoxometalates§

Santiago Reinoso,*[,†] José Ramón Galán-Mascarós,*[,‡] and Luis Lezama[†]

[†]Departamento de Química Inorgánica, Facultad de Ciencia y Tecnología, Universidad del País Vasco (UPV/EHU), P.O. Box 644, 48080 Bilbao, Spain

[‡]Catalan Institution for Research and Advanced Studies (ICREA) and Institute of Chemical Research of Catalonia (ICIQ), Avinguda dels Països Catalans 16, 43007 Tarragona, Spain

Supporting Information

ABSTRACT: The first heterometallic copper−cerium polyoxometalate, $[\{Ce^{IV}(OAc)\}Cu^{II}_3(H_2O)(B\text{-}\alpha\text{-}GeW_9O_{34})_2]^{11-}$ (**1**), is composed of an unprecedented copper(II)-trisubstituted Weakley-type tungstogermanate subunit stabilized by coordination of a $\{Ce(OAc)\}^{3+}$ group at the vacant position. The title species contains a central $\{Ce^{IV}Cu^{II}_3O_{18}\}$ rhomblike cluster that belongs to a new $\{(4f_{ext})(3d_{ext})(3d_{int})_2\}$ type and magnetically behaves as a triangular Cu_3 system with overall antiferromagnetic exchange affected by the structural distortions the vicinity of diamagnetic Ce^{IV} induces.

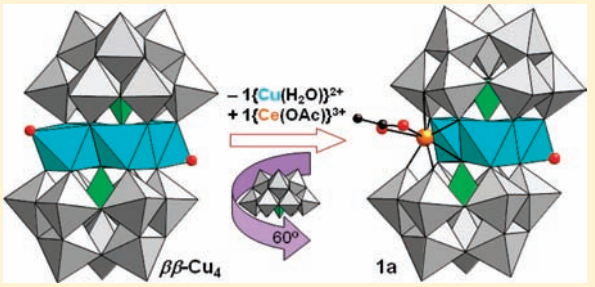

INTRODUCTION

Polyoxometalates (POMs) are anionic clusters composed of O-bridged early transition metals, and they show a remarkable structural variety and a multitude of potential applications (catalysis, materials science, biomedicine, or nanotechnology).[1] Among the numerous POM families, transition-metal-substituted POMs constitute one of the most extensively studied areas owing to their intriguing catalytic/magnetic properties.[2] The use of lacunary POMs as highly nucleophilic, multidentate O-donor ligands has allowed for construction of magnetically well-isolated clusters of paramagnetic d centers with highly diverse nuclearities and topologies, thus representing suitable molecular models for detailed magnetic studies. In contrast, little work has been devoted to heterometallic 3d−4f POMs,[3] so that only a few structurally characterized examples are known.[4]

The much higher reactivity toward POMs of the strongly oxophilic 4f ions with respect to that of the divalent late 3d metals appears to be one of the key factors behind the low number of 3d−4f POMs reported. Different synthetic strategies have been applied to overcome this, such as using preformed heterometallic clusters as precursors in the reaction with lacunary species[4c,d] or introducing exogenous ligands in 3d−4f−POM systems.[4f,g] We decided to investigate an alternative approach consisting of incorporation of 4f ions to 3d-substituted POMs that can behave as lacunary species. Weakley-type dimers[5] appear to be suitable candidates for this purpose. The outer $M(H_2O)$ groups in their central, rhomblike moieties of four edge-sharing MO_6 octahedra are relatively labile, as indicated by the isolation of defect di- and trisubstituted derivatives,[6] which can effectively act as lacunary species and incorporate M′ ions in the vacancies to form mixed 3d clusters.[7]

Recently, we demonstrated that Weakley-type dimers are indeed reactive toward 4f ions by preparing the first heterometallic 3d−4f derivative related to this class of POMs, which contained a central $\{(4f_{ext})_2(3d^{ox}_{int})_2\}$-type rhomblike cluster.[8] Here, we report on the second member of this family, namely, $[\{Ce^{IV}(OAc)\}Cu^{II}_3(H_2O)(B\text{-}\alpha\text{-}GeW_9O_{34})_2]^{11-}$ (**1**), which exemplifies a new type of Weakley-like heterometallic 3d−4f species with a central $\{(4f_{ext})(3d_{ext})(3d_{int})_2\}$ core.

EXPERIMENTAL SECTION

Materials and Methods. The $[Cu^{II}_4(H_2O)_2(B\text{-}\alpha\text{-}GeW_9O_{34})_2]^{12-}$ ($\beta\beta$-Cu_4) polyanion was synthesized following literature procedures,[9] and to be used as the precursor, it was isolated as the potassium salt by bulky precipitation with excess KCl(s). All other chemicals were purchased from commercial sources and used without further purification. Elemental analyses were performed by Ibercron (SGIker, UPV/EHU, Bilbao, Spain). Infrared spectra were obtained as KBr pellets on a Nicolet 5700 FT-IR spectrophotometer. Thermal analysis was carried out from room temperature to 900 °C at a rate of 5 °C/min on a Mettler-Toledo TGA/SDTA 851 thermobalance with a 100 mL/min flow of synthetic air. Magnetic susceptibility measurements on grained single crystals were performed on a Quantum Design MPMS-XL-5 SQUID magnetometer in the 2−300 K range under an applied direct current (dc) magnetic field of 0.1 T. EPR measurements were performed on grained single crystals in the 4−300 K range, and they were registered for X-band studies on a Bruker ELEXSYS 500 spectrometer with a maximum available microwave power of 200 mW and equipped with a superhigh-Q resonator ER-4123-SHQ. For Q-band studies, EPR spectra were recorded on a Bruker EMX system equipped with

Received: June 21, 2011
Published: August 25, 2011

Table 1. Crystallographic Data for Compound 1a

formula	$C_2H_{45}CeCs_3Cu_3Ge_2K_4Na_4O_{91}W_{18}$
fw (g mol^{-1})	5957.7
cryst syst	triclinic
space group	$P-1$
a (Å)	12.5496(2)
b (Å)	17.4025(4)
c (Å)	23.3170(5)
α (deg)	101.966(2)
β (deg)	91.712(2)
γ (deg)	108.183(2)
V (Å^3)	4708.32(17)
Z	2
D_{calcd} (g cm^{-3})	4.202
μ (mm^{-1})	25.097
collected reflns	34 532
unique reflns (R_{int})	14 834 (0.030)
obsd reflns [$I > 2\sigma(I)$]	10 679
parameters	648
$R(F)^a$ [$I > 2\sigma(I)$]	0.046
$wR(F^2)^a$ (all data)	0.138
GoF	1.071

$^a R(F) = \Sigma||F_o| - |F_c||/\Sigma|F_o|$; $wR(F^2) = \{\Sigma[w(F_o^2 - F_c^2)^2]/\Sigma[w(F_o^2)^2]\}^{1/2}$.

an ER-510-QT resonator and an ER-4112-HV liquid helium cryostat. The magnetic field was calibrated by a NMR probe, and the frequency inside the cavity was determined with a Hewlett-Packard 5352B microwave frequency counter.

$Cs_3K_4Na_4[\{Ce^{IV}(C_2H_3O_2)\}Cu^{II}_3(H_2O)(B\text{-}\alpha\text{-}GeW_9O_{34})_2]\cdot\sim 20H_2O$ (1a). Aqueous 0.1 M $Ce(NH_4)_2(NO_3)_6$ (1 mL, 0.10 mmol) was added to a suspension of $K_{12}[Cu_4(H_2O)_2(B\text{-}\alpha\text{-}GeW_9O_{34})_2]$ (0.55 g, 0.10 mmol) in aqueous 0.5 M acetic acid/sodium acetate buffer (20 mL). The reaction mixture was stirred at room temperature for 30 min, and after filtering any solid off, aqueous 1 M CsCl (0.5 mL) was added to the resulting greenish yellow solution. A pale green powder was removed after 1 day, and then the solution was left to slowly evaporate at room temperature. Yellow prisms of **1a** suitable for single-crystal X-ray diffraction were formed after approximately 2 months, when the solution was reduced to a volume of ~3 mL and its color had changed to green (yield 0.17 g, 29% based on Ge). Anal. Calcd (found) for $C_2H_{45}CeCs_3Cu_3Ge_2K_4Na_4O_{91}W_{18}$: Ce, 2.35 (2.30); Cs, 6.69 (6.75); Cu, 3.20 (3.30); Ge, 2.44 (2.43); K, 2.62 (2.66); Na, 1.54 (1.43); W, 55.6 (56.8). IR (cm^{-1}): 946(m), 897(s), 827(m), 817(m), 771(vs), 726 (s), 627(m), 517(w), 487 (w), 447(w). TGA/DTA (Figure SI1 in the Supporting Information): two endothermic processes in the 25−100 °C range and an exothermic process at ~200 °C result in a continuous mass loss involving release of ~21 water molecules and pyrolysis of the acetate group below 370 °C [% calcd for $21H_2O + 1C_2H_3O_2$ (found) 7.34 (7.50)]. Final decomposition is indicated by two overlapping exothermic signals in the 560−620 °C range.

X-ray Data Collection and Crystal Structure Determination. Crystallographic data for compound **1a** are summarized in Table 1. Intensity data for a yellow prism of **1a** mounted in a cryoloop were collected at 120(2) K on an Oxford Diffraction Gemini S diffractometer equipped with graphite-monochromated Mo Kα radiation (λ = 0.71073 Å) and a Sapphire CCD detector. Data collection, unit cell determination, intensity data integration, routine corrections for Lorentz and polarization effects, and multiscan absorption correction were performed using the CrysAlis Pro software package.[10] The structure was solved using SIR2004[11] and refined with SHELXL97.[12] Both programs were integrated in the WinGX software package.[13] Two Cs atoms were disordered over two positions each (Cs2/Cs2A and Cs3/Cs3A), and the population parameters of two Na atoms were refined without restrictions, resulting in fractional occupations. All metal atoms with the exception of Na and K were refined anisotropically. Hydrogen atoms of the methyl group were placed in calculated positions and refined with a riding model using standard SHELXL parameters. Bond valence sum (BVS) calculations[14] were performed with the BVSumCalc program. The final geometrical calculations were carried out with the PLATON program.[15]

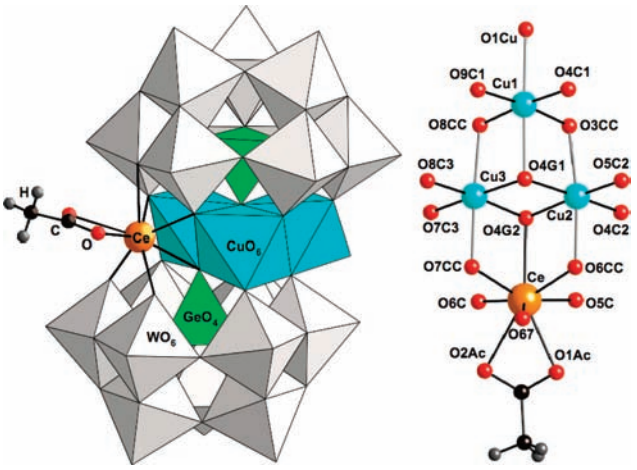

Figure 1. Polyhedral/ball-and-stick representations of **1** (left) and its central $\{Ce^{IV}Cu^{II}_3O_{18}\}$ cluster (right, axial Cu−O bonds in gray).

RESULTS AND DISCUSSION

Synthesis. Recently, we prepared the first Weakley-like heterometallic 3d−4f POM, $[\{Ce^{III}(H_2O)_2\}_2Mn^{III}_2(B\text{-}\alpha\text{-}GeW_9O_{34})_2]^{8-}$, from stoichiometric reaction of Ce^{IV} with $[Mn^{II}_4(H_2O)_2(B\text{-}\alpha\text{-}GeW_9O_{34})_2]^{12-}$ in water. Formation of this species involved substitution of the outer Mn centers by Ce^{III} atoms as a result of Mn^{II} to Mn^{III} oxidation, leading to a $\{(4f_{ext})_2(3d^{ox}_{int})_2\}$-type rhomblike cluster.[8] With the aim of extending these studies to nonoxidizeable Weakley-type POMs, we selected the Cu analogue $[Cu^{II}_4(H_2O)_2(B\text{-}\alpha\text{-}GeW_9O_{34})_2]^{12-}$ ($\beta\beta$-Cu_4)[9] as precursor and explored its reactivity toward the Ce^{IV} oxidant in different conditions of solvent, pH, or temperature. Applying similar synthetic conditions as for our $\{(Ce^{III})_2(Mn^{III})_2\}$ POM we only obtained yellow powders that were unfortunately not possible to characterize adequately. Nevertheless, reaction of the $\beta\beta$-Cu_4 precursor with $Ce(NH_4)_2(NO_3)_6$ (1:1 ratio) in a NaOAc buffer did result in polyanion **1**, which was isolated as the salt $Cs_3K_4Na_4[\mathbf{1}]\cdot\sim 20H_2O$ (**1a**) by direct crystallization with CsCl. The IR spectrum of **1a** (Figure SI2 in the Supporting Information) is very similar in shape to that of $\beta\beta$-Cu_4 with slight 5−10 cm^{-1} blue shifts for all the bands originating from stretching vibration modes, except for the most intense ν_{as}(W−O−W) peak (~775 cm^{-1}). Two new overlapping peaks around 820 cm^{-1} are observed in close analogy to the 820 cm^{-1} peak found for our $\{(Ce^{III})_2(Mn^{III})_2\}$ Weakley-like POM.[8] This constitutes a strong indication of Ce being incorporated to the precursor skeleton and of the sandwich-type framework being retained upon incorporation.

Crystal Structure. Polyanion **1** can be viewed as the product of the substitution of one outer Cu atom in the $\beta\beta$-Cu_4 precursor

dx.doi.org/10.1021/ic201331d |Inorg. Chem. 2011, 50, 9587–9593

Table 2. Selected Bond Lengths (Å) for 1

Cu1 sphere		Cu2 sphere	
Cu1−O4C1	1.945(12)	Cu2−O4C2	1.931(15)
Cu1−O9C1	1.950(15)	Cu2−O5C2	1.946(13)
Cu1−O8CC	1.968(12)	Cu2−O4G1	2.006(14)
Cu1−O3CC	1.971(15)	Cu2−O4G2	2.061(12)
Cu1−O4G1	2.362(10)	Cu2−O6CC	2.303(11)
Cu1−O1Cu	2.370(14)	Cu2−O3CC	2.328(12)
Cu3 sphere		**Ce sphere**	
Cu3−O8C3	1.955(16)	Ce−O6CC	2.190(12)
Cu3−O7C3	1.955(12)	Ce−O6C	2.204(12)
Cu3−O4G1	2.000(11)	Ce−O7CC	2.218(14)
Cu3−O4G2	2.026(14)	Ce−O5C	2.242(15)
Cu3−O7CC	2.325(12)	Ce−O1Ac	2.393(14)
Cu3−O8CC	2.331(11)	Ce−O2Ac	2.483(13)
		Ce−O67	2.516(12)
		Ce−O4G2	2.618(11)

by a $\{Ce(OAc)\}^{3+}$ group, where the capping OAc^- ligand displays a κ^2-O,O′ chelating mode, together with a 60° rotation of one $\{B\text{-}\alpha\text{-}GeW_9O_{34}\}$ fragment (Figure 1). Oxidation states for Ce^{IV} and Cu^{II} atoms are in full agreement with both the number of alkaline cations determined by elemental analyses and the bond valence sum calculations,[14] which also indicate that the O1Cu water molecule is the only protonation site. This leads to a sandwich framework of ideal C_s symmetry, which constitutes the first copper−cerium heterometallic POM known. There are four Cu-containing heterometallic POMs reported so far, but they all belong to a family of Cu_3−4f (4f = La, Gd, Eu) cubane moieties stabilized by monolacunary Keggin fragments,[4f,h] whereas the Ce^{IV}-containing examples are limited to two assemblies based on Ce^{IV}−Mn^{IV} clusters and lacunary Wells−Dawson subunits.[4c,d]

The central $\{Ce^{IV}Cu^{II}_3O_{18}\}$ rhomblike cluster belongs to a new $\{(4f_{ext})(3d_{ext})(3d_{int})_2\}$ type, and it is composed of three Jahn−Teller (JT) distorted octahedra (one external $Cu^{II}O_5(H_2O)$ or Cu_{ext} and two internal $Cu^{II}O_6$ or Cu_{int}) and one $Ce^{IV}O_6(O_2CCH_3)$ square antiprism, all edge sharing (Figure 1). The Ce−O bonding is consistent with other Ce^{IV}-containing POMs,[16] and it can be described as four short and one long bonds with two edge-shared W_2O_{10} dimers, two long Ce−O(Ac) bonds, and one very long Ce−O(Ge) bond (Table 2). The Cu_{int} centers are equatorially bridged by the GeO_4 groups, and the linkages between the Cu_{ext} and Cu_{int} centers are of the equatorial−axial type, so that the axial directions of the three 4 + 2 distorted Cu octahedra are parallely alligned. This is common for all Cu^{II}-substituted Weakley-type POMs[9,17] and the nonaquated αα-derivatives,[18] the disubstituted $[Na_2(H_2O)_2Cu_2(As_2W_{15}O_{56})_2]^{18-}$ POM with equatorial−axial connectivity between Cu_{int} atoms representing the single exception known.[6f]

Rotation of the $\{B\text{-}\alpha\text{-}GeW_9O_{34}\}$ fragment with respect to the precursor skeleton with ββ configuration of the lacunary−central cluster junctions results in the αβ isomer. This configuration is characteristic of trisubstituted Weakley POMs,[7a,g] and thus, **1** can alternatively be described as a Cu^{II}-trisubstituted Weakley-type tungstogermanate stabilized by coordination of a $\{Ce(OAc)\}^{3+}$ group at the vacant position. The assembly of **1** is indeed virtually identical to that of $[NaNi_3(H_2O)_2(XW_9O_{34})_2]^{11-}$ (X = P, As)[6b,d]

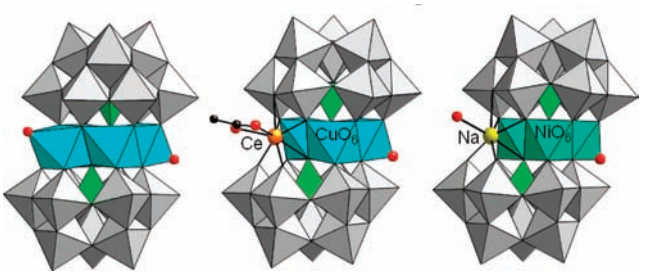

Figure 2. Structural relationship between the ββ-Cu_4 precursor (left), polyanion **1** (center), and the $[NaNi_3(H_2O)_2(XW_9O_{34})_2]^{11-}$ (X = P, As) POMs (right).

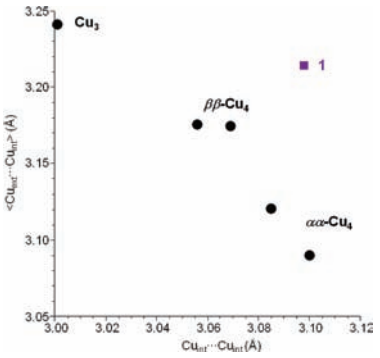

Figure 3. Representation of the mean $Cu_{int}\cdots Cu_{ext}$ distance vs the $Cu_{int}\cdots Cu_{int}$ distance for the copper(II)-substituted tungstogermanates of Table SI1 in the Supporting Information.

with X = Ge^{IV}, Cu^{II} in place of Ni^{II} and Ce^{IV} playing the role of Na^+ (Figure 2). The observation of such subunit is unprecedented because no Weakley-type trisubstituted example with Cu^{II} in the central cluster or Ge^{IV} as heteroatom has been reported to date.

Table SI1 in the Supporting Information displays the Cu bonding parameters of **1** compared to those of Cu^{II}-substituted Weakley-type POMs, nonaquated αα-tungstogermanate derivatives, and the closely related $[Cu_3(H_2O)(\beta\text{-}HGeW_9O_{34})(\beta\text{-}HGeW_8O_{31})]^{12-}$ sandwich-type species (Cu_3).[19] Although showing Cu−O bond lengths and angles comparable to those of the Cu^{II}-tetrasubstituted Weakley POMs, the Cu_{int} octahedra in **1** appear to be relatively less JT elongated, and this can also be noticed when comparing with the Cu_3 and αα-derivatives. The more regular Cu_{int} geometry in **1** is also reflected in slight increases of the Cu···Cu distances and Cu_{int}−O−Cu_{ext} angles with respect to the ββ-Cu_4 precursor. Given the rigidity imposed by the trilacunary ligands, no substantial variations in the Cu geometries could be expected for this type of sandwich frameworks. Nevertheless, Figure 3 reveals that the subtle differences between the Cu···Cu distances for the tungstogermanate POMs seem to be somehow correlated in such a way that the Cu_{int} atoms tend to separate from each other as the mean $Cu_{int}\cdots Cu_{ext}$ distance decreases following the sequence Cu3/ββ-Cu_4/αα-Cu_4. Polyanion **1** is clearly shifted away from this trend: while the $Cu_{int}\cdots Cu_{ext}$ distance is comparable to the Cu_3 sandwich POM with a similar Cu_3O_{13} moiety, the separation between the Cu_{int} atoms falls in the region of the αα-derivatives with square-pyramidal Cu_{ext} atoms displaced from their basal planes toward the apical O(Ge) atoms in the inner part of the

dx.doi.org/10.1021/ic201331d |Inorg. Chem. 2011, 50, 9587–9593

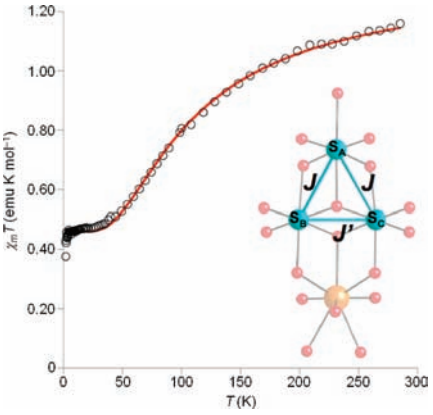

Figure 4. Temperature dependence of the χT product for **1a** (black circles), and scheme for the magnetic superexchange within the $\{Ce^{IV}Cu^{II}_3O_{18}\}$ rhomblike cluster. The continuous line represents the best fit to a triangular model.

POM skeleton. The fact that the $Cu_{int}\cdots Cu_{int}$ distance in **1** is longer than should be expected from this trend can be attributed to a breathing of the POM framework promoted by incorporation of Ce^{IV} in place of a Cu_{ext} atom, showing that Weakley-type POMs can be flexible to some extent when accommodating metal centers with large sizes as 4f ions.

In the absence of any redox action from Ce^{IV} as for our $\{(Ce^{III})_2(Mn^{III})_2\}$ Weakley-like POM,[8] formation of **1** can only be attributed to slow evolution in buffered NaOAc medium of the original tetra- to a final trisubstituted species via release of an outer $Cu(H_2O)$ group and subsequent $\beta\beta$ to $\alpha\beta$ rearrangement, to which a $\{Ce(OAc)\}^{3+}$ group is then incorporated. This is consistent with the long crystallization time compared to the $\{(Ce^{III})_2(Mn^{III})_2\}$ POM. In our case, Ce^{IV} was shown to be an ideal coordinating agent to quench and stabilize the monolacunary POM skeleton formed after isomerization even in the presence of Na^+, which is known to fill the vacant sites in almost all defect Weakley-type POMs reported.[6,7] These observations indicate that 4f ions could be readily incorporated to both mono- or divacant Weakley-type POMs and, therefore, that complete series of heterometallic sandwich POMs comprising $\{(4f_{ext})_2(3d_{int})_2\}$ or $\{(4f_{ext})(3d_{ext})(3d_{int})_2\}$ rhomblike clusters could in principle be designed depending on the availability of unsaturated precursors. Given that oxidation of tetrasubstituted POMs appears to result in disubstituted species with high-valent internal 3d atoms[6a,8] and that disubstituted POMs can selectively uptake only one 3d atom to generate mixed-metal trisubstituted species,[7e] the possibility of synthesizing series of POMs with $\{(4f_{ext})_2(3d^{ox}{}_{int})_2\}$, $\{(4f_{ext})(3d'_{ext})(3d^{ox}{}_{int})_2\}$, or $\{(4f_{ext})(3d'_{ext})(3d_{int})_2\}$ cores could not be disregarded.

Magnetic Properties. The χT product at room temperature is 1.16 emu K mol^{-1} (Figure 4), and it is in good agreement with that expected for a magnetically diluted sample containing three Cu^{II} ions (each one contributing a spin-only value of ~0.33 emu K mol^{-1}); hence, the presence of diamagnetic Ce^{IV} is confirmed.[20] The χT product decreases down to a value of 0.46 emu K mol^{-1} below 40 K, where it reaches a plateau corresponding to the paramagnetic ground state of the Cu_3 trimer. This value remains constant down to 3 K, where an additional decrease is observed, probably due to intermolecular interactions. According to this, the magnetic core in the $\{Ce^{IV}Cu^{II}_3O_{18}\}$ cluster can be described as an isosceles Cu_3 triangle with two different superexchange pathways (inset in Figure 4) and magnetic data can thus be fitted with the following Hamiltonian

$$H = -\sum 2J(S_AS_B + S_AS_C) + 2J'(S_B + S_C)$$

Magnetic data are perfectly reproduced by this model in the 4–300 K range with an overall antiferromagnetic (AF) exchange. This AF interaction is quite stronger in the shorter Cu_B-Cu_C pathway between Cu_{int} atoms ($J' = -68.8$ cm^{-1}) than in the longer Cu_A-Cu_B and Cu_A-Cu_C pathways between Cu_{int} and Cu_{ext} atoms ($J = -23.6$ cm^{-1}), the obtained $g = 2.22$ value being reasonable. These parameters are in good agreement in sign and relative magnitude with those reported for other rhomblike Cu_4O_{16} and triangular Cu_3O_{13} clusters of edge-shared CuO_6 octahedra sandwiched between trilacunary Keggin or Wells–Dawson fragments, as shown in Table 3. Although there are some differences in the absolute values of the AF exchange parameters (J and J'), the J'/J ratio in most of them is very consistent with the differences between the $Cu_{int}\cdots Cu_{int}$ and the $Cu_{int}\cdots Cu_{ext}$ distances. The larger the difference, a larger J'/J ratio would obviously be expected, and this is actually what we observe. Indeed, polyanion **1** shows the minimum J'/J ratio of 2.9 with a difference between the long and the short sides of its isosceles Cu_3 triangle corresponding to just 3.6%. In comparison, J'/J values in the 3–4 range for the Weakley-type species and slightly above 7 for the Cu3 sandwich are observed, and accordingly, the differences in the Cu···Cu distances are noticeably larger, around 5–6% for the former and reaching over 7% for the latter. There is only one exception for this trend in the $Cu_4(GeW_9O_{34})_2$ POM (or $\beta\beta$-Cu_4 precursor), but we do not find any structural justification for this case. The presence of Ce^{IV} should explain the fact of **1** showing the lowest J'/J ratio, since its large size allows for a larger $Cu_{int}\cdots Cu_{int}$ distance and stabilizes longer Cu–O bond lengths for the core atoms as mentioned above. It is also remarkable to note that the magnetic exchange is very sensitive to the nature of the heteroatom, although it does not directly participate in the magnetic pathway. The exchange parameters for the Ge-containing POMs are at about 1 order of magnitude stronger than when P or Si occupy the tetrahedral sites. Variations in the size (Si^{IV} vs Ge^{IV}) or charge (Si^{IV} vs P^V) of the heteroatom do not substantially affect the Cu···Cu distances or Cu–O–Cu angles; hence, these variations in the magnetic exchange must have an electronic origin.

EPR Spectroscopy. X- and Q-band EPR spectra are temperature dependent between 300 and 50 K but remain essentially unchanged down to 4 K (Figure 5). Despite the observed high-temperature broadening, different contributions to the spin Hamiltonian are detected by comparing the signals from both bands, such as fine and hyperfine splitting or the Zeeman electronic term. The room-temperature X-band signals are too broad to extract any information, but many separate lines can be clearly identified on the Q-band spectrum. Besides two intense central lines at ~1025 and 1150 mT, four weaker satellites are also observed (~270, 590, 770, and 1410 mT). As the temperature is lowered, the intensity of the central lines grows and their resolution improves considerably, while the satellites decrease in intensity and become hardly detectable below 50 K, showing that they originate from an excited state. The spectra below 20 K exhibit the features of a Cu^{II} atom with a near axial **g** tensor, in such a way that a quartet hyperfine is clearly detected working at the X band on the parallel component, and this is originated from a spin doublet $S = 1/2$ interacting with a single $I = 1/2$ nucleus (inset in Figure 5). The best-fit results for the spin Hamiltonian parameters of this ground state are $g_{||} = 2.462$, $g_\perp = 2.082$,

dx.doi.org/10.1021/ic201331d |Inorg. Chem. 2011, 50, 9587–9593

Table 3. Cu···Cu Distances (Å) and Exchange Coupling Constants (cm^{-1}) for Rhomblike Cu_4O_{16} and Triangular Cu_3O_{13} Clusters in Sandwich-Type POMs

	Cu_4O_{16}				Cu_3O_{13}	
	$Cu_4(PW_9O_{34})_2$[17a,21]	$Cu_4(SiW_9O_{34})_2$[17c]	$Cu_4(GeW_9O_{34})_2$[9]	$Cu_4(P_2W_{15}O_{56})_2$[17a,21]	1	Cu3 sandwich[19]
$Cu_{int}\cdots Cu_{int}$	3.081(3)	2.965(3)	3.069(2)	3.051(9)	3.097(3)	3.001(3)
$Cu_{ext}\cdots Cu_{int}$	3.245(4)	3.162(3)	3.174(2)	3.219(9)	3.198(3)	3.239(3)
	3.256(4)	3.162(3)	3.176(2)	3.193(9)	3.229(3)	3.243(3)
$\langle Cu_{ext}\cdots Cu_{int}\rangle$	3.250(4)	3.162(3)	3.175(2)	3.206(9)	3.214(3)	3.241(3)
% difference	5.21	6.23	3.34	4.83	3.63	7.40
J	−3.5	−0.1	−11.0	−3.5	−23.6	−6.5
J'	−12.5	−0.3	−82.0	−12.5	−68.8	−47.0
J'/J	3.6	3.0	7.4	3.6	2.9	7.2

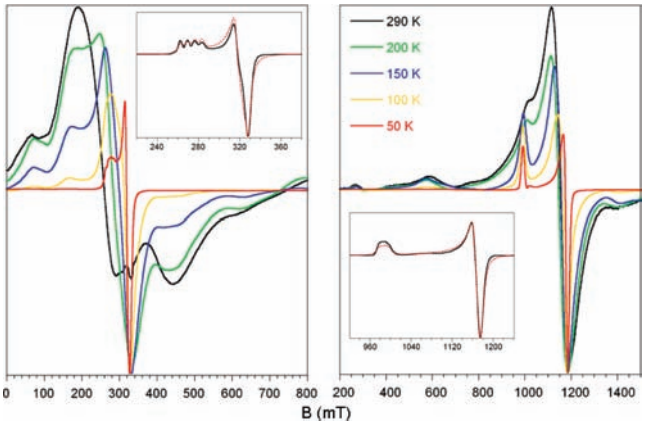

Figure 5. Temperature dependence of the X-band (left) and Q-band (right) EPR spectra for **1a**. (Insets) Low-temperature X-band (left, 5 K) and Q-band (right, 20 K) EPR spectra with red dashed lines representing the best-fitting simulated spectra.

$A_{||} = 80 \times 10^{-4}$ cm^{-1}, and $A_{\perp} < 30 \times 10^{-4}$ cm^{-1},[22] and they are consistent with an unpaired electron located mainly on a $d(x^2-y^2)$ orbital. It is worth noting that certain anisotropy on the perpendicular component has been detected on the Q-band spectrum ($g_1 = 2.468$, $g_2 = 2.088$, $g_3 = 2.074$).

Considering the trimeric magnetic core in **1**, the spectra have been analyzed in terms of three active states with temperature-dependent population, one quartet ($S = 3/2$) and two doublets ($S = 1/2$).[23] The latter can be identified by the intermediate quantum number $S_{BC} = S_B + S_C$. On the basis of the J and J' exchange values obtained from the magnetic data, only the Kramer doublet $|0,1/2\rangle$ should be populated below 20 K, whereas signals corresponding to the transitions inside the $|1,1/2\rangle$ doublet and $|1,3/2\rangle$ quartet could be observed at room temperature (Figure 6). Thus, the satellites above 50 K correspond to transitions within the quartet state, and their effective g values very different from 2 indicate an important zero-field splitting (ZFS) on the $S = 3/2$ term. The higher intensity of the central lines is due to additional contributions of the transitions within the doublets. Our attempts to fit the whole spectrum were unfortunately unsuccessful owing to many transitions occurring at similar fields and each spin state's g values being somewhat different because of the nonequivalence of the Cu ions, but nevertheless, a $|D| < 0.24$ cm^{-1} maximum value can be proposed from the position of the outer lines of the ZFS spectra.

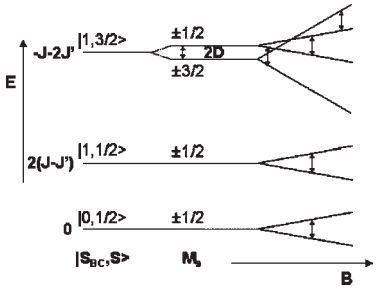

Figure 6. Diagram of energy levels for the three spin states in the magnetic core of **1**.

The four equally spaced hyperfine lines in the low-temperature X-band spectra, showing approximately the same relative amplitude, are characteristic of the $|0,1/2\rangle$ state of an isosceles Cu_3 triangle.[24] A more complicated pattern with 16 lines should be observed for the $|1,1/2\rangle$ doublet, whereas the classic hyperfine spectrum with 10 1:3:6:10:12:12:10:6:3:1 equally spaced peaks (resulting from one unpaired electron interacting with three equivalent $I = 3/2$ nucleus) is expected for the $|1,3/2\rangle$ quartet. Assuming no transitions between different Kramer doublets, the hyperfine splitting should be strongly dependent on the temperature, the J and J' values, and the J'/J ratio in such a way that hyperfine structures from all states are simultaneously produced with small exchange values and a J'/J ratio close to unity, and this causes loss of the resolution in the spectra. However, the four hyperfine lines must theoretically be observed in a certain temperature range when the exchange values are moderate and appreciably different. In fact, this pattern has also been described for the low-temperature spectra of a spin-frustrated, equilateral Cu_3 triangle.[25] The observation at low temperature of such type of signal for **1** indicates that the $|0,1/2\rangle$ doublet constitutes the ground state and that it is well isolated from the excited doublet and quartet, thus supporting the J and J' values determined from magnetic measurements. It is also worth mentioning that the g and A values determined by fitting this signal correspond to the Cu_A external atom.[26]

CONCLUSIONS

The first heterometallic copper−cerium polyoxometalate, $[\{Ce^{IV}(OAc)\}Cu^{II}_3(H_2O)(B\text{-}\alpha\text{-}GeW_9O_{34})_2]^{11-}$, has been prepared by stoichiometric reaction of $[Cu^{II}_4(H_2O)_2(B\text{-}\alpha\text{-}GeW_9O_{34})_2]^{12-}$ with Ce^{IV} in buffered medium, confirming that

dx.doi.org/10.1021/ic201331d |Inorg. Chem. 2011, 50, 9587–9593

4f ions are ideal coordinating agents to quench and stabilize lacunary Weakley-type POM fragments generated in situ not only from oxidation of parent POMs but also from slow transformation in solution of nonoxidizeable precursors as in the present work. This has allowed for isolation of a Weakley-type trisubstituted subunit with Cu^{II} in the central cluster or Ge^{IV} as heteroatom for the first time. The central $\{Ce^{IV}Cu^{II}{}_3O_{18}\}$ cluster of the title polyanion exemplifies a new type of heterometallic 3d−4f rhomblike core, namely, $\{(4f_{ext})(3d_{ext})(3d_{int})_2\}$, and magnetically behaves as a an isosceles Cu_3 triangle with an overall antiferromagnetic exchange that, according to magnetic susceptibility and EPR studies, is affected by the structural distortions (such as the increase of the $Cu_{int}\cdots Cu_{int}$ distance), incorporation of the large, diamagnetic Ce^{IV} in an external site promotes. Extension of this work to other parent or lacunary Weakley-type precursors and 4f ions to systematically analyze magnetic properties in complete series of POMs with $\{(4f_{ext})_2(3d^{ox}{}_{int})_2\}$, $\{(4f_{ext})_2(3d_{int})_2\}$, or $\{(4f_{ext})(3d_{ext})(3d_{int})_2\}$ cores is in progress.

■ ASSOCIATED CONTENT

Supporting Information. Cu bonding parameters of **1** compared to closely related Cu^{II}-substituted sandwich-type POMs (Table SI1); TGA curve, IR spectrum, and X-ray crystallographic data in cif format for **1a**. This material is available free of charge via the Internet at http://pubs.acs.org.

■ AUTHOR INFORMATION

Corresponding Author

*E-mail: santiago.reinoso@ehu.es (S.R.); jrgalan@iciq.es (J.R. G.-M.).

Funding Sources

Ministerio de Ciencia e Innovación (MICINN)

■ ACKNOWLEDGMENT

The authors thank P. Vitoria (UPV/EHU) for crystallographic discussions and Dr. M. H. Dickman for the BVSCalc program. Financial support by MICINN is acknowledged: Grant CTQ2008-03197/BQU and Juan de la Cierva research contract (to S.R.).

■ DEDICATION

§Dedicated to the memory of my father, Benedicto Reinoso Rodríguez (1946−2011).

■ REFERENCES

(1) (a) Pope, M. T. *Heteropoly and Isopoly Oxometalates*; Springer-Verlag: Berlin, Germany, 1983. (b) In *Polyoxometalates: From Platonic Solids to Antiretroviral Activity*; Pope, M. T., Müller, A., Eds.; Kluwer: Dordrecht, The Netherlands, 1994. (c) In *Polyoxometalate Chemistry: From Topology via self-Assembly to Applications*; Pope, M. T., Müller, A., Eds.; Kluwer: Dordrecht, The Netherlands, 2001. (d) In *Polyoxometalate Chemistry for Nanocomposite Design*; Pope, M. T., Yamase, T., Eds.; Kluwer: Dordrecht, The Netherlands, 2002. (e) In *Polyoxometalate Molecular Science*; Borrás-Almenar, J. J., Coronado, E., Müller, A., Pope, M. T., Eds.; Kluwer: Dordrecht, The Netherlands, 2003. (f) Pope, M. T. In *Comprehensive Coordination Chemistry II*; McCleverty, J. A., Meyer, T. J, Eds.; Elsevier Ltd.: Oxford, U.K., 2004.

(2) (a) Hill, C. L.; Prosser-McCartha, C. M. *Coord. Chem. Rev.* **1995**, *143*, 407. (b) Clemente-Juan, J. M.; Coronado, E. *Coord. Chem. Rev.* **1999**, *193*−*195*, 361. (c) Kortz, U.; Müller, A.; van Slageren, J.; Schnack, J.; Dalal, N. S.; Dressel, M. *Coord. Chem. Rev.* **2009**, *253*, 2315.

(3) Reinoso, S. *Dalton Trans.* **2011**, *40*, 6610.

(4) (a) Xue, G.; Liu, B.; Hu, H.; Yang, J.; Wang, J.; Fu, F. *J. Mol. Struct.* **2004**, *690*, 95. (b) Merca, A.; Müller, A.; van Slageren, J.; Läge, M.; Krebs, B. *J. Cluster Sci.* **2007**, *18*, 711. (c) Fang, X.; Kögerler, P. *Chem. Commun.* **2008**, 3396. (d) Fang, X.; Kögerler, P. *Angew. Chem., Int. Ed.* **2008**, *47*, 8123. (e) Chen, W.; Li, Y.; Wang, Y.; Wang, E.; Zhang, Z. *Dalton Trans.* **2008**, 865. (f) Nohra, B.; Mialane, P.; Dolbecq, A.; Rivière, E.; Marrot, J.; Sécheresse, F. *Chem. Commun.* **2009**, 2703. (g) Yao, S.; Zhang, Z.; Li, Y.; Lu, Y.; Wang, E.; Su, Z. *Cryst. Growth Design* **2010**, *10*, 135. (h) Wang, W.-D.; Li, X.-X.; Fang, W.-H.; Yang, G.-Y. *J. Cluster Sci.* **2011**, *22*, 87. (i) Zhang, Z.-M.; Li, Y.-G.; Yao, S.; Wang, E.-B. *Dalton Trans.* **2011**, *40*, 6475.

(5) (a) Weakley, T. J. R.; Evans, H. T., Jr.; Showell, J. S.; Tourné, G. F.; Tourné, C. M. *J. Chem. Soc., Chem. Commun.* **1973**, 139. (b) Finke, R. G.; Droege, M. W. *Inorg. Chem.* **1983**, *22*, 1006.

(6) (a) Zhang, X.; Anderson, T. M.; Chen, Q.; Hill, C. L. *Inorg. Chem.* **2001**, *40*, 418. (b) Kortz, U.; Mbomekalle, I. M.; Keita, B.; Nadjo, L.; Berthet, P. *Inorg. Chem.* **2002**, *41*, 6412. (c) Ruhlmann, L.; Canny, J.; Contant, R.; Thouvenot, R. *Inorg. Chem.* **2002**, *41*, 3811. (d) Mbomekalle, I. M.; Keita, B.; Nierlich, M.; Kortz, U.; Berthet, P.; Nadjo, L. *Inorg. Chem.* **2003**, *42*, 5143. (e) Kortz, U.; Hamzeh, S. S.; Nasser, N. A. *Chem.—Eur. J.* **2003**, *9*, 2945. (f) Anderson, T. M.; Fang, X.; Mbomekalle, I. M.; Keita, B.; Nadjo, L.; Hardcastle, K. I.; Farsidjani, A.; Hill, C. L. *J. Cluster Sci.* **2006**, *17*, 183. (g) Hou, Y.; Xu, L.; Cichon, M. J.; Lense, S.; Hardcastle, K. I.; Hill, C. L. *Inorg. Chem.* **2010**, *49*, 4125.

(7) (a) Anderson, T. M.; Zhang, X.; Hardcastle, K. I.; Hill, C. L. *Inorg. Chem.* **2002**, *41*, 2477. (b) Mbomekalle, I. M.; Keita, B.; Nadjo, L.; Neiwert, W. A.; Zhang, L.; Hardcastle, K. I.; Hill, C. L.; Anderson, T. M. *Eur. J. Inorg. Chem.* **2003**, 3924. (c) Ruhlmann, L.; Canny, J.; Vaissermann, J.; Thouvenot, R. *Dalton Trans.* **2004**, 794. (d) Mbomekalle, I. M.; Cao, R.; Hardcastle, K. I.; Hill, C. L.; Amman, M.; Keita, B.; Nadjo, L.; Anderson, T. M. *C. R. Chimie* **2005**, *8*, 1077. (e) Ruhlmann, L.; Costa-Coquelard, C.; Canny, J.; Thouvenot, R. *J. Electroanal. Chem.* **2007**, *603*, 260. (f) Ruhlmann, L.; Costa-Coquelard, C.; Canny, J.; Thouvenot, R. *Eur. J. Inorg. Chem.* **2007**, 1493. (g) Mbomekalle, I. M.; Mialane, P.; Dolbecq, A.; Marrot, J.; Sécheresse, F.; Berthet, P.; Keita, B.; Nadjo, L. *Eur. J. Inorg. Chem.* **2009**, 5194.

(8) Reinoso, S.; Galán-Mascarós, J. R. *Inorg. Chem.* **2010**, *49*, 377.

(9) Kortz, U.; Nellutla, S.; Stowe, A. C.; Dalal, N. S.; Rauwald, U.; Danquah, W.; Ravot, D. *Inorg. Chem.* **2004**, *43*, 2308.

(10) *CrysAlis Pro*, version 3; Oxford Diffraction, Ltd.: Oxford, U.K., 2009.

(11) Burla, M. C.; Caliandro, R.; Camalli, M.; Carrozzini, B.; Cascarano, G. L.; De Caro, L.; Giacovazzo, C.; Polidori, G.; Spagna, R. *J. Appl. Crystallogr.* **2005**, *38*, 381.

(12) Sheldrick, G. M. *Acta Crystallogr.* **2008**, *A64*, 112.

(13) Farrugia, L. J. *J. Appl. Crystallogr.* **1999**, *32*, 837.

(14) Brown, I. D.; Altermatt, D. *Acta Crystallogr.* **1985**, *B41*, 244.

(15) Spek, A. L. *Acta Crystallogr.* **2009**, *D65*, 148.

(16) See, for example: Sousa, F. L.; Almeida Paz, F. A.; Cavaleiro, A. M. V.; Klinowski, J.; Nogueira, H. I. S. *Chem. Commun.* **2004**, 2656.

(17) (a) Weakley, T. J. R.; Finke, R. G. *Inorg. Chem.* **1990**, *29*, 1235. (b) Bi, L.-H.; Huang, R.-D.; Peng, J.; Wang, E.-B.; Wang, Y.-H.; Hu, C.-W. *J. Chem. Soc., Dalton Trans.* **2001**, 121. (c) Kortz, U.; Isber, S.; Dickman, M. H.; Ravot, D. *Inorg. Chem.* **2000**, *39*, 2915. (d) Zhang, Z.; Yao, S.; Wang, E.; Shi, Q.; Zhang, H. *J. Cluster Sci.* **2008**, *19*, 521. (e) Bi, L.-H.; Wang, E.-B.; Peng, J.; Huang, R.-D.; Xu, L.; Hu, C.-W. *Inorg. Chem.* **2000**, *39*, 671.

(18) (a) Yamase, T.; Abe, H.; Ishikawa, E.; Nojiri, H.; Ohshima, Y. *Inorg. Chem.* **2009**, *48*, 138. (b) Chen, L.; Zhang, L.; Gao, Y.; Pang, L.; Xue, G.; Fu, F.; Wang, J. *J. Coord. Chem.* **2009**, *62*, 2832.

(19) Nsouli, N. H.; Ismail, A. H.; Helgadottir, I. S.; Dickman, M. H.; Clemente-Juan, J. M.; Kortz, U. *Inorg. Chem.* **2009**, *48*, 5884.

(20) Harrison, W. T. A.; Reis, K. P.; Jacobson, A. J.; Schneemeyer, L. F.; Waszczak, J. V. *Chem. Mater.* **1995**, *7*, 2161.
(21) Gómez-García, C. J.; Coronado, E.; Borrás-Almenar, J. J. *Inorg. Chem.* **1992**, *31*, 1667.
(22) These parameters were estimated by comparison with those obtained from the following computer simulation program working at the second order of perturbation theory: *WINEPR-SimFonia*, version 1.25; Bruker Analytische Messtechnik GmbH: Karlsruhe, Germany, 1996.
(23) (a) Mukherjee, P.; Drew, M. G. B.; Estrader, M.; Díaz, C.; Ghosh, A. *Inorg. Chim. Acta* **2008**, *361*, 161. (b) Liu, X.; de Miranda, M. P.; McInnes, E. J. L.; Kilner, C. A.; Halcrow, M. A. *Dalton Trans.* **2004**, 59. (c) Yoon, J.; Solomon, E. I. *Coord. Chem. Rev.* **2007**, *251*, 379.
(24) Belinsky, M. I. *Inorg. Chem.* **2004**, *43*, 739.
(25) Cage, B.; Cotton, F. A.; Dalal, N. S.; Hillard, E. A.; Rakvin, B.; Ramsey, C. M. *J. Am. Chem. Soc.* **2003**, *125*, 5270.
(26) Bencini, A.; Gatteschi, D. *EPR of Exchange-Coupled Systems*; Springer: Berlin, 1990.